Experimental and analytical investigation of dynamic crack patterns in automotive windshield sheets subjected to low velocity impact

P. Shojaei Shahmirzadi, H. Saeidi Googarchin*

Automotive Fluids and Structures Analysis Research Laboratory, School of Automotive Engineering, Iran University of Science and Technology, Tehran 16846-13114, Iran

*Corresponding Author : hsaeidi@iust.ac.ir

Abstract

Off-road cars' windshields are vulnerable to different types of stones, road debris and pebbles due to common off paved and gravel surfaces in which they drive. Any attempt to design windshield that minimizes injury and death of occupants during a vehicle accident requires a thorough understanding of the mechanical behavior of automotive windshield subjected to foreign object impact loads.

In this study, some drop ball tests in different impact energy levels are conducted in order to monitor fracture behavior of an off-road automotive windshield. Also dynamic crack patterns of laminated glasses are examined based on the impact energy levels and impact conditions. In addition, the acceleration which is imposed to impactor during the accident is recorded. The experimental results are compared to an analytical approach regarding the resultant impact force as well. There is a good agreement between the impact forces of experimental test results and analytical approaches ones. All in all, in low velocity impacts, impact energy releases through powdering region in impact area, radial cracks and strain energy in PVB. It is concluded that in lower impact energy levels, the higher impact speed, the more number of radial cracks. In addition, at higher energy levels, number of radial cracks decease due to higher strain energy levels in PVB interlayer. Therefore, in low velocity impacts, number of radial cracks has reverse relationship with penetration depth in PVB interlayer.

Keywords: *automotive windshield- drop ball test -analytical approach -Impact fracture behavior · dynamic crack pattern.*

Introduction

The automotive windshield impact to foreign objects such as a pedestrian's head is one of the most fundamental safety issues to car makers due to lethal consequences of the resultant acceleration for the pedestrian. Hence, the acceleration of the object should not exceed a certain limit. In addition, the passengers should be protected from the broken windshield after an accident. This fact gives rise to a question whether how a windshield should response to different impact energy levels. Unfortunately, in the case of the cars which are capable of driving on and off paved or gravel surfaces , little effective modification and improvement has been made on the response of their windshields to impacts. As a matter of fact, their windshields are prone to different types of stones since vehicle tires usually pick up and throw pebbles.

Experimental tests are efficient methods for observing real cases which are possible to happen in practice. Several experimental studies have been carried out in the literature to investigate the behavior of laminated glass under dynamic loading conditions.

The function of PVB is to keep the layers of glass bonded even when broken (due to the adhesiveness of the interlayer). Therefore glass fragments are still firmly bonded to PVB interlayer after the impact to reduce the scratched danger. Cracks on the laminated windshield contains a great deal of accident information [1], therefore accident reconstruction analysis by extracting useful information from the cracks of

the laminated windshield is of great interest for current research.

Timmel et al. [2] conducted a four-point bending test, in which the experimental setup consisted of a laminated glass plate (total thickness: 6.72 mm, 0.72 mm PVB) bearing/ supported by two cylinders to evaluate three different material models in explicit FE solver (LS-DYNA) as well as fit the best material model with experiment data to describe the behavior of the PVB laminated glass. Muralidhar et al. [3] and Rahulkumar et al. [4] used a compressive shear strength experiment to study the debonding phenomenon occurring in the glass polymer interface.

In the case of dynamic investigations, Charpy, drop-weight tests and the Split Hopkinson Pressure Bar (SHPB) or Kolsky's apparatus have been widely used. [5]

Many researchers have used drop ball tests in low velocity impacts to examine responses of monolithic and laminated structures against impact. Chai et al. observed the propagation of cracks in layered glass from low-velocity impact of sharp or spherical tip projectiles using high-speed photography. Drop ball tests were also carried out to determine the threshold impact energy for chipping in glass blocks and subsurface crack instability in an edge-supported glass plates. [6], [7], [8], [9].

Theoretical approach for cracked plates

Seshadri et al. [5] derived a theoretical approach for the purpose of post-fracture analysis.

They avoided the problem of determining the fragmentation pattern and took it as given. In the analytical study, the cracks were assumed to be radial and the glass fragments triangular in shape.

Further, in developing a theoretical model, it was assumed all fragments to be identical.

The aim was to capture the main features of the response of a cracked laminate without using the details of the crack pattern. The formulas for a regular n-sided polygon cracked into n identical triangular fragments, simply supported at the edges and displaced at the center, with n>3 can be condensed as:

$$\frac{F}{l(2\Gamma_0 Eh)^{1/2}} = n\left(\sin^2(\frac{\pi}{n})\tan(\frac{\pi}{n})\frac{(\delta_0/l)}{\sqrt{1-(\delta_0/l)^2}} + \sin(\frac{\pi}{n})\cos(\frac{\pi}{n})\frac{\delta_0}{l}\right) \quad (1)$$

As the number of fragments becomes very large, this relation can be approximated as:

$$\frac{F}{l(2\Gamma_0 Eh)^{1/2}} = n\frac{\delta_0}{l} + \frac{\pi^3(\delta_0/l)}{n^2(1-(\delta_0/l)^2)^{1/2}} \quad (2)$$

Where Γ_0 is the fracture energy, E is elastic modulus, h is the thickness of the polymer layer, l is distance between center of specimen and edge of cracked part, δ_0 is the center displacement, F is the maximum force.

Experimental procedure

The experiments were conducted on a drop ball testing machine (shown in Fig.1) equipped with accelerometer to investigate the laminated glass temporal response after the impact of a hard sphere. Some other specifications of the machine are shown in Table 1.

The geometrical and mechanical properties of the impactor (which is depicted in Fig.2) are explained in Table 2.

The PVB Common windscreen testing methodologies are widely used by windscreen manufacturers. Windscreen manufacturers ensure the quality of the windscreens by testing them to various standards.

Table 1. Some specifications of drop ball test machine

Dropping height range	data acquisition frequency
0.1m to 3m	76923 Hz

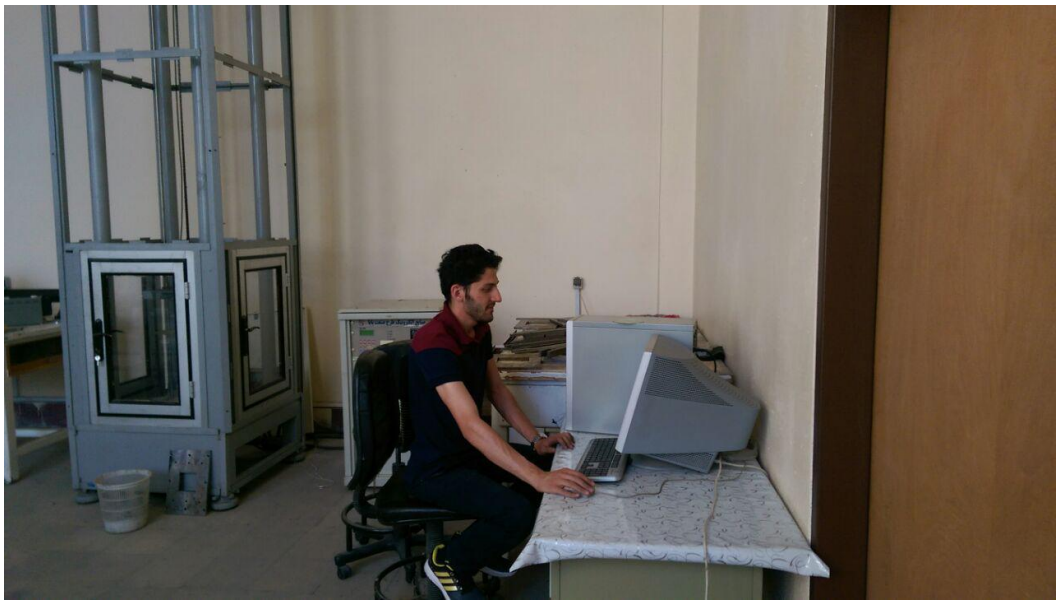

Fig1. Drop ball test machine used for experimental tests

Table 2. Properties of the imp actor

Geometrical properties	Mechanical properties
Spherical part: Diameter= 16mm	Material: steel
Cylindrical part: Height 45mm	E= 200GPa, μ=0.3

Fig2. Steel imp actor used in drop ball tests

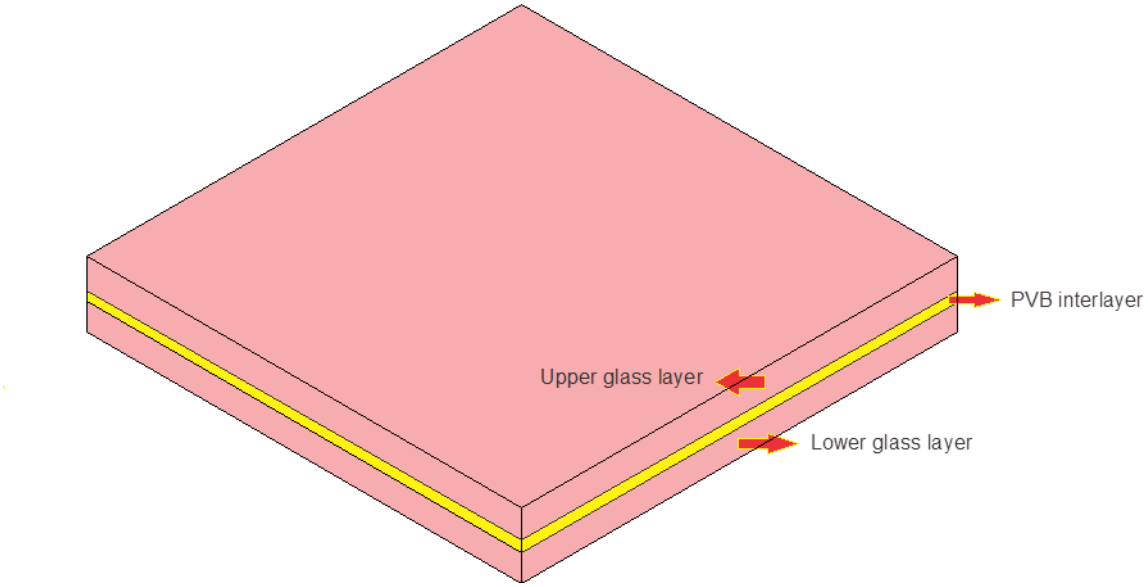

Fig3. Schematic picture of laminated glass specimen

Table 3. Initial conditions of drop ball tests

Test Code	Height (m)	Impact Velocity (m/s)	Impactor mass (kg)	Impact Energy (J)
D-B-T-1	0.2	1.980	2.0511	4.024
D-B-T-2	0.2	1.980	2.0511	4.024
D-B-T-3	0.25	2.214	2.712	6.651
D-B-T-4	0.4	2.801	2.0511	8.049
D-B-T-5	0.75	3.836	2.0511	15.09
D-B-T-6	1	4.429	2.712	26.60

These test methodologies involve dropping steel balls of varying diameters from varying heights onto windscreen glass samples under controlled conditions. The drop-ball methodologies are widely used, well documented and are included in a number of standards for windscreen testing. A drop test is similar across a number of these standards. The Australian Standard – Safety glass for land vehicles - AS/NZS 2080:1995 describes two tests involving dropping a steel ball onto a flat windscreen sample 305 ± 5mm square. [10]

Due to limitation in x and y coordinates of the drop ball test machine, the laminated glass specimen used in the experiment is a square flat plate with the dimension of 25cm×25cm×0.6cm shown in Fig.3. These samples were cut from the windshield of an off-road automotive. The reason why this kind of windshield was chosen stems from the fact that off-road cars are more vulnerable to stones and pebbles which are thrown from the gravel surfaces. In the experiment specimens, the PVB interlayer is 1 mm thick sandwiched by two sheets of 2.5 mm-thick soda-lime glass. The laminated glass specimen is fixed by two steel frames, with a rubber interlayer between the specimen and the frame in order to avoid the damage of the specimen and eliminate the residual stress. The vertical impact load is applied in the center of the specimen by the impactor. The end part of the impactor is equipped with an impact head which

can be designed into different shapes. In this study, we use the hemispherical shape of the impact head. Samples were fully clamped in all experiments. Initial conditions of all drop ball tests are given in Table3. The procedure of tests is sorted based on increasing the impact energy.

Results and discussion

Laminated glass specimen after test code D-B-T-1 is shown in Fig.4.

As it is observed from Fig.4, the impact region at the center of specimen is a circle with approximate diameter of 3mm. Indeed, due to low energy of impact, the impactor has not caused remarkable damage at the impact area. In addition, the impactor has not penetrated in the specimen and damage is superficial. As a matter of fact, the impact energy has been released through radial cracks propagation and the impactor has not had any penetration in the specimen.

It can be inferred from Fig.4 that the radial cracks in test code D-B-T-1 are nearly symmetrical and about 67 from which this quantity, 60 cracks have been extended to the borders of specimen and released their energy through reaching the boarder pf specimen. As a consequence, the damage mode is dynamic crack propagation. In this specimen, no circumferential crack is observed which can be due to low level of impact energy. Consequently, it seems that although all the impact procedure occurs in less than some milliseconds, radial cracks are made at the first stage. At the vicinity of impact region, some sectors of circles are observed which are distributed sporadically to the approximate radius of 6mm from the center of specimen. Moreover it can be seen from Fig.4 that the radial cracks have been propagated from the impact surface of laminated glass. On the other hand, the radial cracks in this specimen are superficial and have not reached the lower surface of specimen, hence it can be understood that the fracture of laminated glass begins with superficial cracks at the upper surface of specimen.

Radial cracks converge at the center of the specimen and its divergence increases at larger radiuses. The acceleration versus time graph of test code D-B-T-1 is illustrated in Fig.5. As it can be inferred from the graph, the maximum acceleration imposed to projectile is 138.4115 m/s^2 which is occurred at 1.34E-03s.

Fig4..specimen after test code D-B-T-1

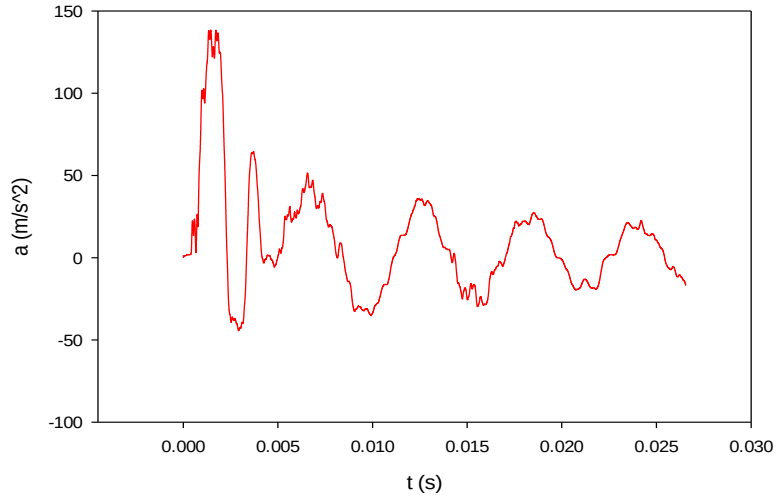

Fig5. Time variations of acceleration for steel impactor in test code D-B-T-1

Fig6..specimen after test code D-B-T-2

Laminated glass specimen after test code D-B-T-2 is shown in Fig.6

Like test code D-B-T-1, no circumferential crack is observed at the specimen. The results of this test are akin to the test code D-B-T-1, just 2 differences are observed:

There are 62 radial cracks which is five number less than test code D-B-T-1.

The damage region at the center of specimen in test code D-B-T-2 is a bit larger than the counterpart region in test code D-B-T-1.

Indeed, some part of failure mode has been transformed to powdering failure mode. Generally speaking, these differences are trivial and can be neglected. It can be concluded that test code D-B-T-1 and D-B-T-2 which had similar input variables have shown identical results. The acceleration versus time graph of test code D-B-T-2 is illustrated in Fig.7. As it can be inferred from the graph, the maximum acceleration imposed to projectile is 162.1094 m/s^2 which is occurred at 1.69E-03s.

Laminated glass specimen after test code D-B-T-3 is shown in Fig.8.

As it is observed from Fig.8, the impact region at the center of specimen (powdering

region) is a circle with approximate diameter of 20mm in which cracks density and consequently damage level is higher than the other regions of specimen. There are 5 circumferential cracks in the specimen at the radiuses of 25,30,35,45 and 100mm from the center of the laminated glass sample. After drawing a comparison between this test (test code D-B-T-3) and test code D-B-T-4 it can be concluded that due to boundary influences farther circumferential cracks occur first, then closer cracks start to propagate. Moreover, the radial cracks have been initiated from the impact surface and propagated through the thickness of laminated glass. Also it can be seen from the laminated glass that the radial cracks in test code D-B-T-3 are nearly symmetrical and about 62. Except one side of the specimen, all of the radial cracks have reached the borders of specimen. It is observed that diagonal asymmetrical net shaped cracks have been made. In addition, it can be inferred that the depth of penetration at the center of specimen is trivial and no damage is seen at PVB interlayer. At both upper and lower glass layers, radial cracks of test code D-B-T-3 converge at the center of the specimen and their divergence increases at larger radiuses. The acceleration versus time graph of test code D-B-T-3 is illustrated in Fig.8. As it can be inferred from the graph, the maximum acceleration imposed to projectile is 724.6094m/s^2 which is occurred at 0.000218s.

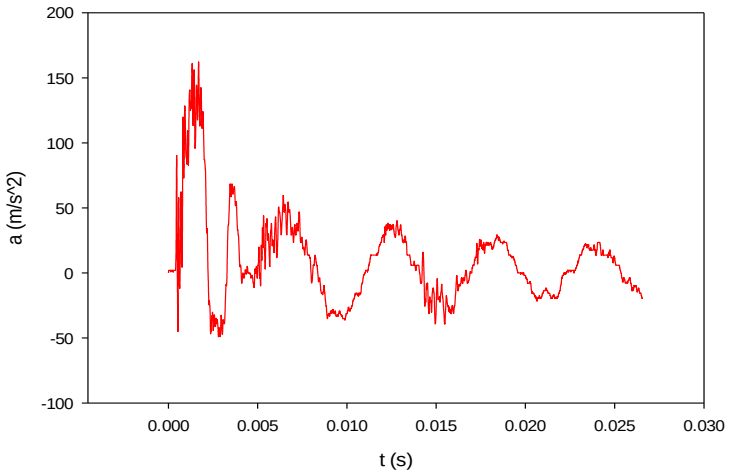

Fig7..Time variations of acceleration for steel impactor in test code D-B-T-2

Fig8. specimen after test code D-B-T-3

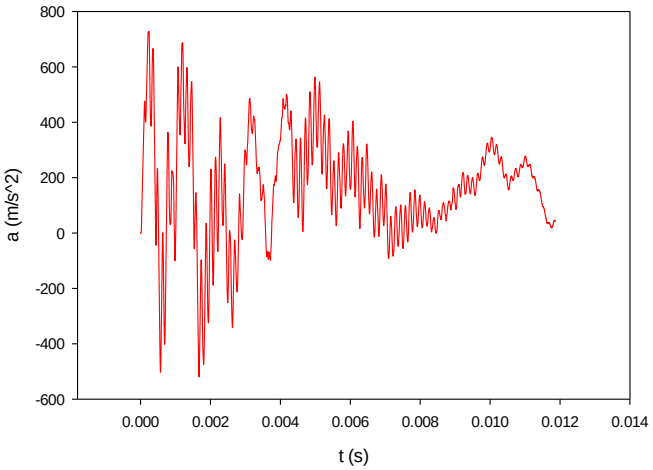

Fig9. Time variations of acceleration for steel impactor in test code D-B-T-3

Fig10. .specimen after test code D-B-T-4

Laminated glass specimen after test code D-B-T-4 is shown in Fig.10.

As it is observed from Fig.10, the impact region at the center of specimen (powdering region) is a circle with approximate diameter of 20mm in which cracks density and consequently damage level is higher than the other regions of specimen. The projectile has penetrated to the depth of 1-1.5mm of the laminated glass and due to 2.5mm thickness of glass layers, no elongation has been occurred in PVB interlayer. Although energy level of test code D-B-T-4 is higher than test code D-B-T-3's one, penetration at the center of specimen is less in test code D-B-T-4 which can be representative of impactor's mass influence. In test code D-B-T-4, the impactor mass is 2.0511kg, while it is 2.0712kg in test code D-B-T-3, therefore it can be concluded that in 2 similar conditions, the less impactor mass, the less penetration depth at the center of specimen.

It is easily seen from test code D-B-T-4 specimen that cracks have initiated from the impact surface and propagated through thickness. In this test, one circumferential crack has been propagated which is at the radius of 95mm from the center. Besides, some sectors of circumferential cracks have been made at the

radiuses of 62, 70 and 80mm from the center of specimen and serve as bridges to connect radial cracks. Also it can be seen from the laminated glass that the radial cracks in test code D-B-T-4 are nearly symmetrical and about 84. After drawing a comparison between test code D-B-T-4 and test code D-B-T-3, it is obvious that radial cracks of test code D-B-T-4 are more than their counterparts in test code test code D-B-T-3, on the other hand circumferential cracks of test code D-B-T-3 are more than test code D-B-T-3's ones. At test code D-B-T-4, distance between radial cracks is shorter than its corresponding item in test code D-B-T-3.

At all 4 sides of specimen which was clamped during the test, diagonal asymmetrical net shaped cracks have been made which have created some right triangles in margins of the specimen. Diagonal net shaped cracks at the margins of test code D-B-T-4 specimen are more congested in comparison to the whole radial cracks. In addition, at both upper and lower glass layers, radial cracks converge at the center of the specimen and their divergence increases at larger radiuses. The acceleration versus time graph of test code D-B-T-3 is illustrated in Fig.11. As it can be seen from the graph, the maximum acceleration imposed to projectile is 732.0356m/s^2 which is occurred at 0.000131s.

Laminated glass specimen after test code D-B-T-5 is shown in Fig.12.

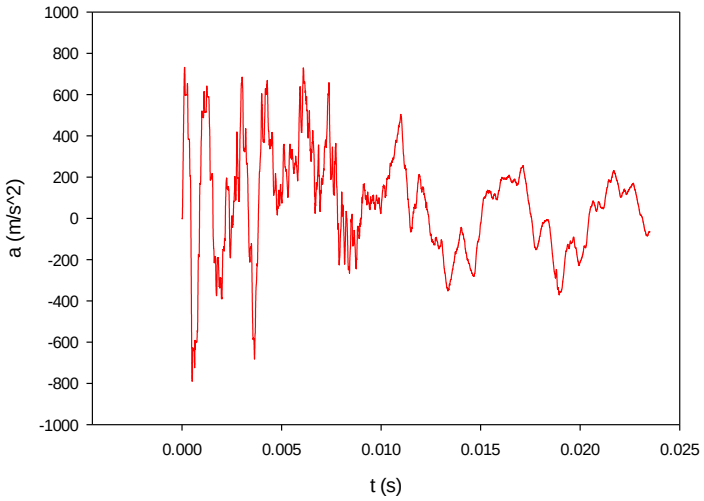

Fig11. Time variations of acceleration for steel impactor in test code D-B-T-4

Fig12. .specimen after test code D-B-T-5

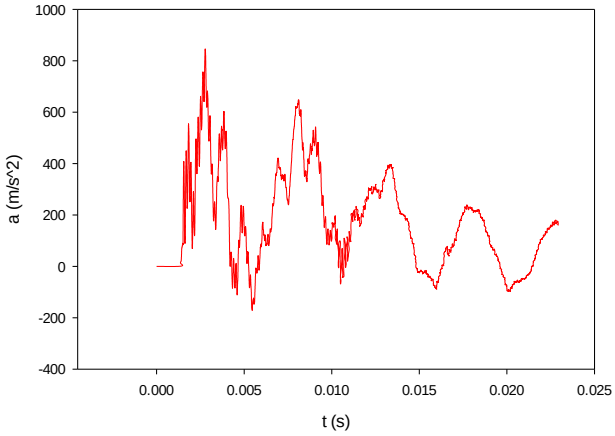

Fig13. .Time variations of acceleration for steel impactor in test code D-B-T-5

Fig14. .specimen after test code D-B-T-6

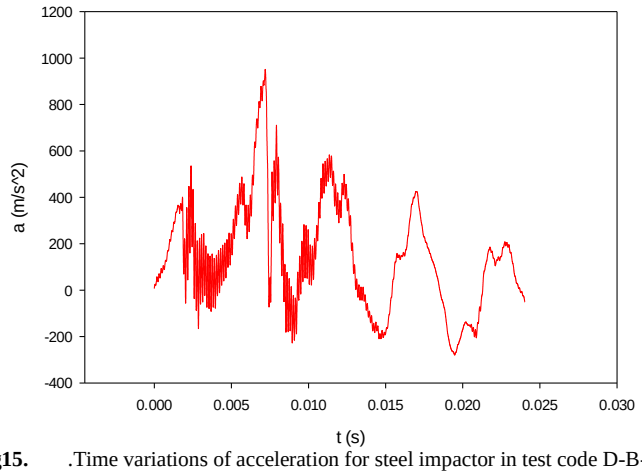

Fig15. .Time variations of acceleration for steel impactor in test code D-B-T-6

As it is observed from Fig.12, the impact region at the center of specimen (powdering region) is a circle with approximate diameter of 20mm in which cracks density and consequently damage level is higher than the other regions of specimen. The projectile has penetrated to the depth of 4mm of the laminated glass, indeed the upper layer glass has fractured and PVB interlayer has elongated, but no tearing is observed. At the center of test code D-B-T-5 laminated glass, penetration depth has increased in comparison to test codes D-B-T-4 and D-B-T-3. Total number of circumferential cracks of the specimen is 5 which are placed at 47, 70, 80, 90 and 105mm distance from the center. At the vicinity of borders (close to clamping spots), net shaped diagonal cracks are more congested. Cracks have been propagated from the impact surface of laminated glass. At all 4 sides of the specimen, diagonal asymmetrical net shaped cracks have been made. At both upper and lower glass layers, radial cracks converge at the center of the specimen and their divergence increases at larger radiuses. Most of radial cracks have reached the borders of specimen and released their internal impact energy by this way.

The acceleration versus time graph of test code D-B-T-5 is illustrated in Fig.13. As it can be inferred from the graph, the maximum acceleration imposed to projectile is 844.140625m/s^2 which is occurred at 0.002782s.

Laminated glass specimen after test code D-B-T-6 is shown in Fig.14.

As it is observed from Fig.14, the impact region at the center of specimen (powdering region) is a circle with approximate diameter of 20mm in which cracks density and consequently damage level is higher than the other regions of specimen. In this test, the projectile has penetrated thoroughly in specimen. Therefore the glass layers have fractured and the PVB interlayer has torn. This test (test code D-B-T-6) has higher impact energy level in comparison to test code D-B-T-5. It can be observed that the penetration at the center of test code D-B-T-6 specimen is deeper than test code D-B-T-5, on the other hand the number of radial cracks is smaller in test code D-B-T-6. In fact, the impact energy has been released mostly through penetration in thickness direction and residual energy has released through radial and circumferential cracks. The radial cracks in test code D-B-T-6 are nearly symmetrical and about 24 which has decreased about 20% in comparison to test code D-B-T-5, but the penetration depth has

increased about 50%. It shows that approximate 76% increase in impact energy level in test code D-B-T-6 in comparison to test code D-B-T-5, has been released mostly through increase in penetration depth and radial and circumferential cracks in further priorities.

There are 6 circumferential cracks in the specimen at the radiuses of 34,41,51,60, 70 and 95mm from the center of the laminated glass sample. It can be seen from Fig.14 that the radial cracks have been initiated from the impact surface of laminated glass and propagated along thickness direction. In one side of the laminated glass, sectors of circumferential cracks like grids, have connected radial cracks to each other. 12 out of total 24 radial cracks have extended to the borders of the specimen and released their internal impact energy by this way. The acceleration versus time graph of test code D-B-T-6 is illustrated in Fig.15

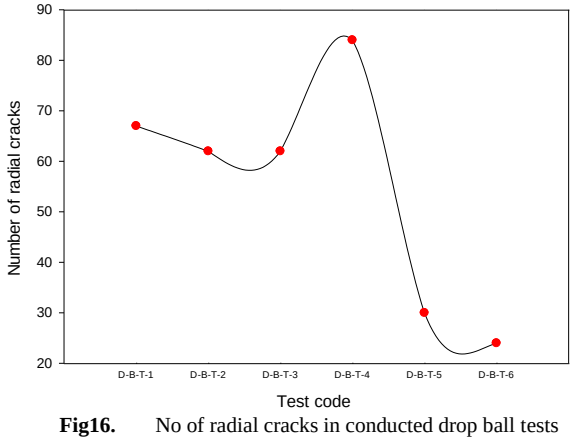

Fig16. No of radial cracks in conducted drop ball tests

Table 4. Penetration depth and total number of radial cracks in drop ball tests

Test Code	Penetration Depth at the center of specimen	Number of Radial Cracks
D-B-T-1	0.1mm	67
D-B-T-2	0.1mm	62
D-B-T-3	0.5mm	62
D-B-T-4	1.25mm	84
D-B-T-5	4mm	30
D-B-T-6	6mm	24

Table 5. Input values of Equation1 and Equation2

Test code	l	Γ_0	E	h	n	δ_0
D-B-T-3	$l=0.025m$	$\Gamma_0=4\frac{J}{m^2}$	$E=74.4GPa$	$h=1mm$	$n=62$	$\delta_0=0.022m$
D-B-T-4	$l=0.095m$	$\Gamma_0=4\frac{J}{m^2}$	$E=74.4GPa$	$h=1mm$	$n=84$	$\delta_0=0.018m$
D-B-T-5	$l=0.1m$	$\Gamma_0=4\frac{J}{m^2}$	$E=74.4GPa$	$h=1mm$	$n=30$	$\delta_0=0.020m$
D-B-T-6	$l=0.034m$	$\Gamma_0=4\frac{J}{m^2}$	$E=74.4GPa$	$h=1mm$	$n=24$	$\delta_0=0.030m$

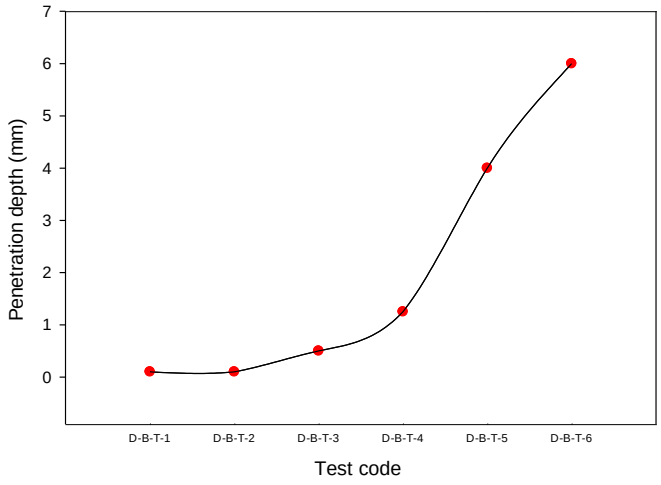

Fig17. Penetration depth in conducted drop ball tests

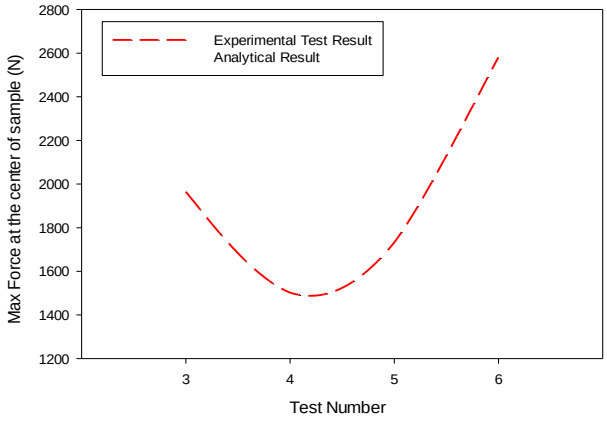

Fig18. Comparison between experimental test and analytical approach in terms of maximum force at the center of specimen

As it can be observed from the graph, the maximum acceleration imposed to projectile is 951.6927m/s^2 which is occurred at 0.00719. Briefly, the penetration depth and number of radial cracks in conducted drop ball tests are shown in Table 4

In addition, Number of radial cracks versus test code No is shown in Fig. 16. Also penetration depth graph at the center of specimens in different drop ball tests is shown in Fig.17

The acceleration and corresponding maximum force of impactor have been calculated by the theoretical formulas and compared with experimental tests. As it is shown in Fig.18 there is a good agreement between the experimental test results and theoretical approach in terms of maximum force which is imposed to impactor.

Conclusion

In this paper, dynamic crack propagation in an off-road automotive windshield sheets was investigated experimentally through drop ball tests. Ten different impact conditions were designed including different impactor mass and dropping height. Further, experimental result was compared to an analytical approach regarding resultant impact force in impactor. Comparison shows a good agreement between the maximum impact force which is induced in impactor during the test and derived from the analytical formulas.

All in all, in low velocity impacts, impact energy releases through powdering region in impact area, radial cracks and strain energy in PVB. It is concluded that in lower impact energy levels, the higher impact speed, the more number of radial cracks. In addition, at higher energy levels, number of radial cracks decease due to higher strain energy levels in PVB interlayer. Therefore, in low velocity impacts, number of radial cracks has reverse relationship with penetration depth in PVB interlayer.

References

[1] C. X. L. Y. Xu, "Modeling and Experimental Studies of Crack Propagation in Laminated Glass Sheets," SAE international journal of materials and manufacturing, vol. 7, no. 2, pp. 328-336, 2014.

[2] K. Timmel, "A finite element model for impact simulation with laminated glass," International Journal of Impact Engineering, vol. 34, pp. 1465-1478, 2007.

[3] J. Muralidhar, "Mechanical behaviour in tension of cracked glass bridged by an elastomeric ligament," Acta Material, vol. 48, pp. 4577-4588, 2000.

[4] J. Rahul, "Interfacial failures in a compressive shear strength test of glass/polymer laminates," International journal of solid structures, vol. 37, pp. 7281-7305, 2000.

[5] S. B. A. J. S. S. M. Seshadri, "Mechanical response of cracked laminated plates," Acta Materialia, vol. 50, p. 4477–4490, 2002.

[6] K. Belingardi, "Design Optimization and Implementation of Composite and Recyclable Thermoplastic Materials for Automotive Bumper," International Journal of Impact Engineering, vol. 27, pp. 213-229, 2002.

[7] A.-S. Aretxabaleta, "Characterisation of the impact behaviour of polymer thermoplastics," Polymer, vol. 24, pp. 145-151, 2005.

[8] L. Liu, "Drop-weight impact tests and finite element modeling of cast acrylic plates," Polymer Testing, vol. 28, pp. 599-611, 2009).

[9] R. Chai, "On the mechanics of fracture in monoliths and multilayers from low-velocity impact by sharp or blunt-tip projectiles," Impact Engineering, vol. 36, pp. 375-385, 2009.

[10] J. Spathonis, "Report on testing to determine impact resistance of vehicle windscreens – overpass screening project," The State of Queensland, Department of Main Roads, Brisbane, 2001.